

Adsorption of Calcium Particles on A36 Mild Steel and its Thermodynamic Parameters

Ezekiel Neza¹, Ayodeji Ayoola^{1*}, Rasheed Babalola² and Bamidele Durodola³

¹Chemical Engineering Department, Covenant University, Ota, Nigeria

²Chemical/Petrochemical Engineering Department,
Akwa Ibom State University, Nigeria

³Chemistry Department, Covenant University, Ota, Nigeria

*Corresponding author: ayodeji.ayoola@covenantuniversity.edu.ng

Received 09/06/2022; accepted 30/09/2022

<https://doi.org/10.4152/pea.2024420201>

Abstract

Adsorption behavior of Ca particles obtained from SS, PS and ES calcination, as well as its Td parameters, during A36 MS coating via phosphating process, was investigated. A36 MS coupons surfaces were coated with phosphates and varied C of Ca particles (from 1 to 2.5 g/dm³), at a T of 60 and 80 °C. Ca particles (as inhibitor) adsorption onto the MS surface obeyed Freundlich's isotherm, with R² values around 1. K_{ads} and Td parameters, such as ΔG, ΔH and ΔS, were also determined. A36 MS coated with Ca particles obtained from calcined SS gave the best A capacity, as revealed in terms of K_{ads}, ΔG and ΔS values. Higher K_{ads} was obtained when T increased from 60 to 80 °C. Also, Td parameters results revealed that Ca particles adsorption mechanism on MS was a more spontaneous process, at an increased T of 80 °C.

Keywords: adsorption; Ca particles; corrosion; MS; Td.

Introduction*

Due to its excellent mechanical qualities and cost effectiveness, MS is commonly utilised for the construction or production of a wide range of engineering materials. However, MS wide areas of applications in engineering exposes it to corrosion, especially in acidic and alkaline environments [1-2]. There are different techniques for metal surfaces coating against corrosion. The choice of a suitable method for a particular metallic material of interest depends upon certain factors, such as the metal nature, corrosive environment, T and inhibitors application methods. [3-4]. Research findings have shown that metals surfaces, such as Zn, Al, Mn, Fe and MS, can be effectively protected using phosphating technique [5]. Phosphating process can be defined as a metallic protective treatment with insoluble phosphate, in order to obtain a reasonably hard and electrically non-conducting metal surface. Phosphate coating is very contiguous and highly adherent to the underlying metal [6]. This technique can also be adopted as a metallic pretreatment step, before the introduction of other protection methods such as lubrication, chemical spraying or painting. Phosphating, a chemical coating process, is cost-effective and has a natural bonding effect. It also gives high anti-corrosion properties. Generally,

* The abbreviations and symbols definitions lists are in page 99.

phosphating has been used in automobile, electronic/electrical and cold processing industries, among others [7].

A thin crystalline layer of phosphate compounds from the phosphate bath sticks to the metal substrate. Recent research has shown that Ca particles addition to coating materials resulted in excellent metal surface protection, due to a more uniform distribution of the fine grains, and improved bonding against corrosion [8-9]. To reduce the cost involved in Ca modified phosphating, pure Ca can be obtained from the processing of waste materials that are rich in carbonates, such as oyster, PS, SS and ES, and animal bones [10].

The coating of metal surfaces by Ca modified phosphating is based on the adsorption process. That is, Ca and phosphates particles are adsorbed onto a metal surface, thereby inhibiting the corrosion process [11-12].

The novelty of this study was to produce pure Ca particles from locally source waste materials. Additionally, it established a suitable adsorption isotherm (and Td parameters) for Ca particles adsorbed during A36 MS coating by phosphates, at two different T (60 and 80 °C) and Ca C from 1 to 2.5 g/L.

Materials and methods

Preparation of the metal coupons

The metal employed in this study was A36 MS. MS coupons were cut into dimensions of 2.8 x 2.8 cm, and polished by various grits of emery paper (P150, 320, 600 and 800). The polished MS coupons surface gained a smooth and homogenous texture, thus ensuring a uniform coating [6].

Calcination of Ca materials

The locally sourced materials used were SS, PS and ES. They were washed thoroughly with water, in order to remove impurities, dried (ES inner membrane was removed), and grinded into particles of $\leq 70 \mu\text{m}$. The ground particles were calcined separately using a muffle furnace (SHI-204 VM), at 800 °C, for 4 h, in order to obtain CaO, through CaCO_3 decomposition [7]. All CaO samples obtained from the three sources were well protected in an air tight closed container, before their application.

A36 MS samples coating

Each of the MS samples was completely dipped into the Zn phosphating bath solution for surface coating. Table 1 shows the coating bath composition (CaO was the only variable parameter). The experimental design of the process is shown in Table 2. Ca amounts adsorbed onto the MS samples were registered.

Table 1. Composition of the coating bath solution.

Reagents	C
ZnO	5 g/L
Zn(NO ₃)	0.2 g/L
NaNO ₃	0.1 g/L
Sodium saccharin	0.1 - 0.2 g/L
CaO	1.0, 1.5, 2.0, 2.5 g/L
H ₃ PO ₄	20 mL/L

Table 2. Experimental design on the phosphating sequence.

T	CaO coating time and C			
T ₁	t ₁ C ₁	t ₁ C ₂	t ₁ C ₃	t ₁ C ₄
	t ₂ C ₁	t ₂ C ₂	t ₂ C ₃	t ₂ C ₄
	t ₃ C ₁	t ₃ C ₂	t ₃ C ₃	t ₃ C ₄
	t ₄ C ₁	t ₄ C ₂	t ₄ C ₃	t ₄ C ₄
T ₂	t ₁ C ₁	t ₁ C ₂	t ₁ C ₃	t ₁ C ₄
	t ₂ C ₁	t ₂ C ₂	t ₂ C ₃	t ₂ C ₄
	t ₃ C ₁	t ₃ C ₂	t ₃ C ₃	t ₃ C ₄
	t ₄ C ₁	t ₄ C ₂	t ₄ C ₃	t ₄ C ₄
T ₃	t ₁ C ₁	t ₁ C ₂	t ₁ C ₃	t ₁ C ₄
	t ₂ C ₁	t ₂ C ₂	t ₂ C ₃	t ₂ C ₄
	t ₃ C ₁	t ₃ C ₂	t ₃ C ₃	t ₃ C ₄
	t ₄ C ₁	t ₄ C ₂	t ₄ C ₃	t ₄ C ₄

T₁, T₂ and T₃ = 40, 60 and 80 °C; C₁, C₂, C₃ and C₄ = 1.0, 1.5, 2.0 and 2.5 g/dm³; t₁, t₂, t₃ and t₄ = 30, 40, 50 and 60 min.

Ca particles adsorption onto the MS surface

MS coupons were immersed in a Ca modified phosphating bath solution (using reagents shown in Table 1). The C of Ca adsorbed onto the MS surface, in the experimental setups, was determined through AAS. The obtained data were subjected to different isotherms (Temkin's, Langmuir's and Freundlich's), in order to establish an appropriate model to describe Ca adsorption behaviour onto the MS surfaces. Freundlich's isotherm was found suitable for Ca adsorption behaviour, and is given in Eq. (1):

$$\log \theta = \log K_{ads} + n \log C_{ads} \quad (1)$$

where θ is in mg/g, n is Freundlich's isotherm and C_{ads} is the C of Ca adsorbed onto the coated MS surface, in mg/g. $\log \theta$ vs. $\log K_{ads}$ plot gives Freundlich's isotherm slope and $\log K_{ads}$ intercept. K_{ads} value was obtained from $\log K_{ads}$ equated to the plot intercept value. The plot gave a straight line from the line with the best model established from the one that produced R^2 value equal or close to one.

Td parameters of Ca particles adsorption onto the MS surface

Using the data obtained from Freundlich's isotherm plot, change in ΔG was evaluated using Van't Hoff's Eq.:

$$\Delta G = -RT \ln(55.5 K_{ads}) \quad (2)$$

Further parameters, such as ΔS and ΔH , were determined using Eq. (3), as given by [10].

$$\ln K_{ads} = \frac{-\Delta H}{RT} + \frac{\Delta S}{R} \quad (3)$$

where R is the universal gas constant (8.314 kJ/kmol/k) and T is operating temperature. From a plot of $\ln K_{ads}$ vs $\frac{1}{T}$ (Eq. 3), $\frac{-\Delta H}{RT}$, when equated to the slope, gave ΔH value. Then, ΔS was calculated from $\frac{\Delta S}{R}$, when equated to the intercept obtained from the plot.

Results and discussion

Calcination result

Table 3 shows the chemical composition of the calcined local materials that produced CaO high content. The results revealed that they were all rich in CaO,

within a range from 79.49 to 84.02 wt%. CaO obtained from the SS had the highest value of 84.02 wt%.

Table 3. Chemical compositions (%) of the locally sourced calcined CaO- rich materials.

Samples	SiO ₂	Al ₂ O ₃	Fe ₂ O ₃	MnO	CaO	P ₂ O ₅	K ₂ O	TiO ₂	SO ₃	Na ₂ O	MgO	RbO	ZnO	Cr ₂ O ₃	SrO	NiO
Snail shell particles	4.25	2.50	2.20	0.40	84.02	0.75	0.52	0.35	1.03	0.002	3.05	0.03	0.10	0.01	0.02	0.08
Periwinkle shell particles	6.95	2.59	2.40	0.42	81.60	0.55	0.30	0.15	1.20	0.002	3.07	0.01	0.01	0.04	0.50	0.03
Egg shell particles	0.41	0.06	0.01	0.02	79.49	0.02	0.05	0.47	0.09	0.16	1.09	0.00	0.00	0.00	0.00	0.00

Ca particles adsorption onto the MS

In order to establish Ca adsorption performance onto the MS surface, Langmuir's, Temkin's and Freundlich's isotherms were employed. Using Eq. (1), a straight line graph was obtained with a plot of $\log \theta$ vs $\log K_{ads}$, which was in accordance with Freundlich's isotherm assumption [13], since the obtained results showed that this model best fit the adsorption phenomenon, with R^2 values close to 1, as shown in Figs. 1-6. That is, Freundlich's adsorption isotherm plots, in order to coat the MS surface, gave various R^2 values for Ca particles obtained from: SS, 0.9194 and 0.9621 (Figs. 1 and 2); PS, 0.7850 and 0.9878 (Figs. 3 and 4); and ES, 0.9036 and 0.7770 (Figs. 5 and 6).

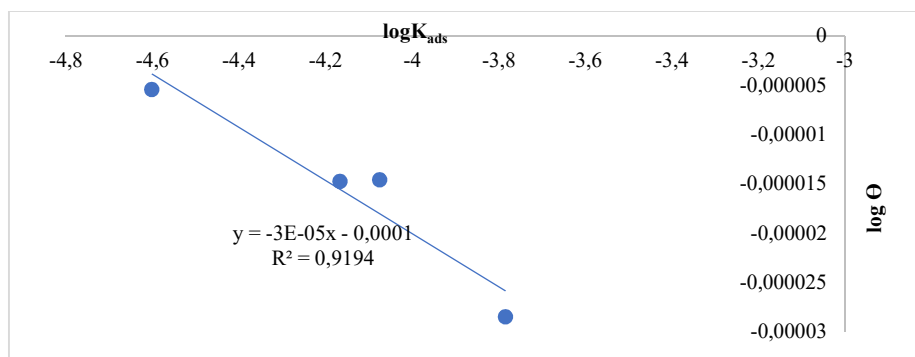


Figure 1. Freundlich's isotherm plot for Ca (using CaO from SS particles) adsorbed onto the MS surface, at 60 °C.

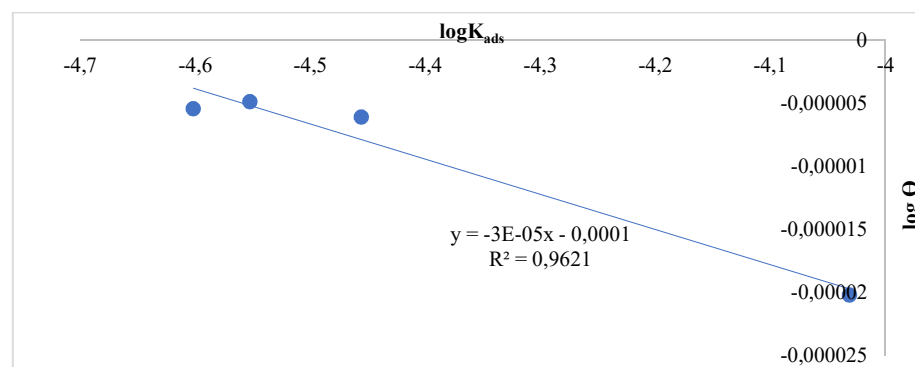


Figure 2. Freundlich's isotherm plot for Ca (using CaO from SS particles) adsorbed onto the MS surface, at 80 °C.

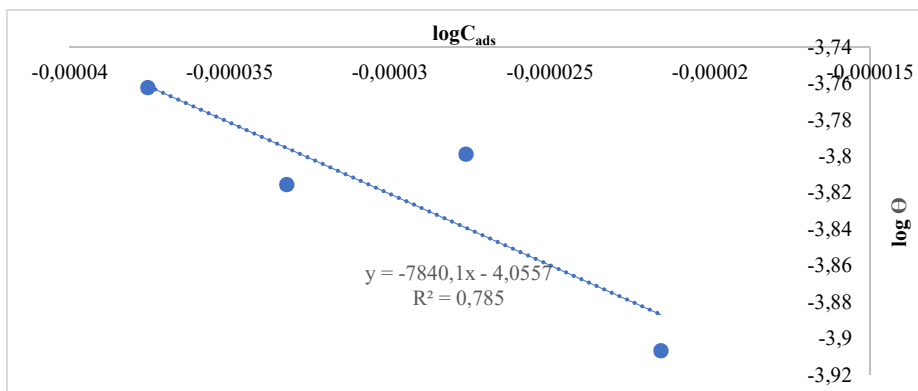


Figure 3. Freundlich's isotherm plot for Ca (using CaO from PS particles) adsorbed onto the MS surface, at 60 °.

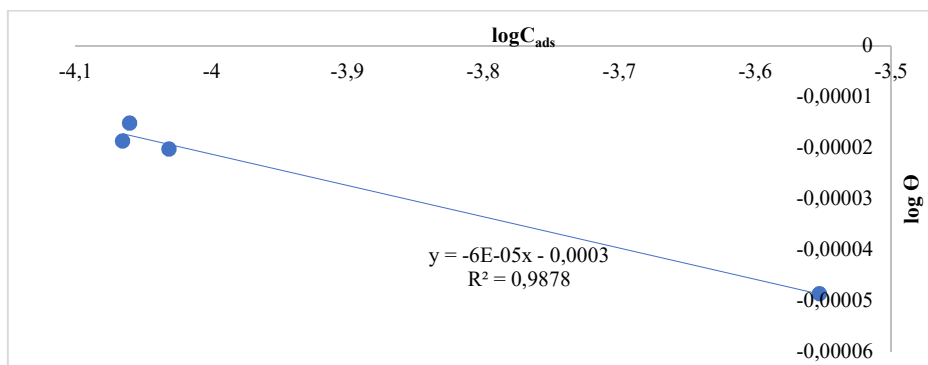


Figure 4. Freundlich's isotherm plot for Ca (using CaO from PS particles) adsorbed onto the MS surface, at 80 °C.

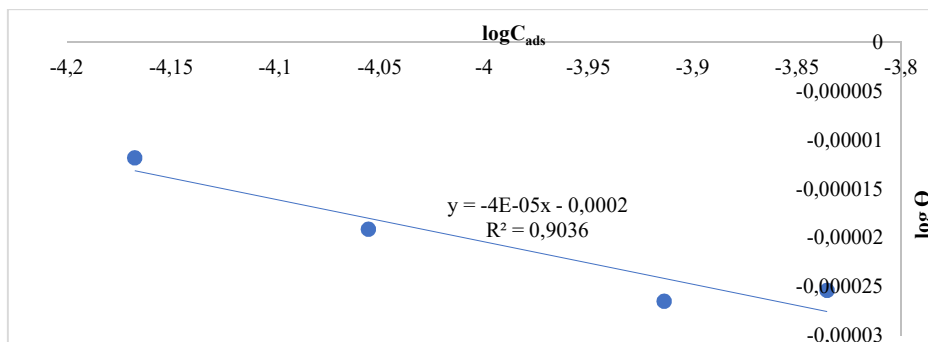


Figure 5. Freundlich's isotherm plot for Ca adsorbed (using CaO from ES particles) onto the MS surface, at 60 °C.

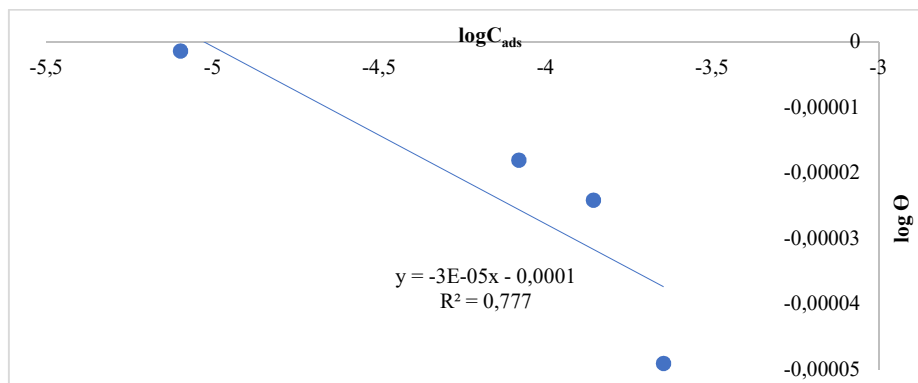


Figure 6. Freundlich's isotherm plot for Ca adsorbed (using CaO from ES particles) on the MS surface, at 80 °C.

K_{ads}

Table 4 shows Td properties of Ca particles adsorption process onto the MS surface. Obtained K_{ads} values were positive, which implied that Ca was adsorbed on the MS surface. From Table 4, Ca from SS particles had the highest obtained K_{ads} values (0.9997). According to [9], larger K_{ads} values indicate higher adsorption tendency [14]. This means that Ca ions from SS particles were more strongly adsorbed onto the MS surface than the other ones.

Table 4. Td parameters (ΔG , ΔS and K_{ads}) from Ca adsorbed onto MS.

Materials	T K/°C	K_{ads}	ΔG (kJ/mol)	ΔS (kJ/K)
St ₃ C ₃ , St ₄ C ₃ ,	333/60	0.99977	-11119.0	0.0017
St ₃ C ₄ , St ₄ C ₄	353/ 80	0.99977	-11786.8	
Pt ₃ C ₃ , Pt ₄ C ₃ ,	333/ 60	0.99909	14734.9	1292.6610
Pt ₃ C ₄ , Pt ₄ C ₄	353/ 80	0.99931	-11785.4	
Et ₃ C ₃ , Et ₄ C ₃ ,	333/ 60	0.99954	-11118.3	0.0299
Et ₃ C ₄ , Et ₄ C ₄	353/ 80	0.99917	-11786.8	

S = CaO from SS; P = CaO from PS; E = CaO from ES

Change in ΔG

The change in ΔG for the adsorption process was calculated using K_{ads} values derived from Freundlich's isotherm (Eq. 2). Changes in ΔG are shown in Table 4. Negative ΔG values showed a spontaneous nature of the adsorption process, and stability of the adsorbed Ca ions onto the coated A36 MS surface. The results revealed that, with an increase in T (from 60 to 80 °C), lower ΔG values were attained. This means that stronger adsorption occurred at higher T [15], since particles gained more energy to migrate at 80 °C. However, there was a deviation in the result of changes in ΔG obtained during Ca particles adsorption, when PS particles were employed at 60 °C.

 ΔS changes

ΔS changes obtained using Eq. (3) were reported in Table 4. Calculated ΔS gave a positive value in each case, that is, the adsorbed Ca ions degree of disorderliness increased [15-16]. Hence, a spontaneous adsorption process occurred in all cases, which confirmed results from K_{ads} and ΔG . Obtained ΔS values were due to the different amount of energy absorbed from the surroundings [9].

Conclusions

The present study concluded that Freundlich's isotherm fitted experimental data for Ca ions adsorbed during MS coating process. Ca particles from SS particles had the strongest adsorption capacity, as revealed in terms of calculated K_{ads} , ΔG and ΔS values. Higher K_{ads} was obtained during the adsorption process, as T increased from 60 to 80 °C. Td parameters results (K_{ads} , ΔG and ΔS) revealed that Ca particles adsorption onto MS was a more spontaneous process at increased T.

Declarations of interest

The authors declare no conflict of interest in this reported work.

Authors' contributions

Ezekiel Neza: provided the original draft, methodology and investigation. **Ayodeji Ayoola:** provided conceptualization, original draft, methodology, investigation, supervision, reviewing and editing. **Rasheed Babalola:** provided conceptualization, reviewing and editing. **Bamidele Durodola:** provided conceptualization, methodology and investigation.

Abbreviations

AAS: atomic absorption analysis
C: concentration
CaCO³: calcium carbonate
ES: egg shells
IE(%): inhibition efficiency
K_{ads}: adsorption equilibrium constant
H₃PO₄: phosphoric acid
MS: mild steel
PS: periwinkle shells
R²: determination coefficient
SS: snail shells
T: temperature
Td: thermodynamic
ZnO: zinc oxide
Zn(NO₃): zinc nitrate

Symbols definition

ΔG: Gibbs free energy
ΔH: change in enthalpy
ΔS: change in entropy
θ: degree of surface coverage

References

1. Chakravarthy MP, Mohana KN. Adsorption and corrosion inhibition characteristics of some nicotinamide derivatives on mild steel in hydrochloric acid solution. *Int Scholar Res Notic.* 2014;(9):1-13. <https://doi.org/10.1155/2014/687276>
2. Wang H L, Liu R B, Xin J. Inhibiting effects of some mercapto-triazole derivatives on the corrosion of mild steel in 1.0 M HCl medium. *Corros Sci.* 2004;(46):2455-2466. <https://doi.org/10.1016/j.corsci.2004.01.023>
3. Cano E, Pinilla P, Polo J L et al. Copper corrosion inhibition by fast green, fuchsin acid and basic compounds in citric acid solution. *Mat Corros.* 2003;(54):222-228. <https://doi.org/10.1002/maco.200390050>
4. Abd El-Maksoud SA. The effect of organic compounds on the electrochemical behaviour of steel in acidic media- A review. *Int J Electrochem Sci.* 2008;(3):528-555.
5. Noor EA, Al-Moubaraki AH. Thermodynamic study of metal corrosion and inhibitor adsorption processes in mild steel/1-methyl-4 [4'(-X)-styryl

- pyridinium iodides/hydrochloric acid systems. *Mat Chem Phys.* 2008;(110):145-154. <http://dx.doi.org/10.1016/j.matchemphys.2008.01.028>
6. Pastorkova J, Jackova M, Pastorek F et al. Effect of phosphating temperature on surface properties of manganese phosphate coating. *Komunikacie.* 2020;(22):55-61. <https://doi.org/10.26552/com.c.2020.1.55-61>
 7. Agbabiaka OG, Oladele IO, Akinwekomi AD et al. Effect of calcination temperature on hydroxyapatite developed from waste poultry eggshell. *Sci Afr.* 2020;(8):e00452. <https://doi.org/10.1016/j.sciaf.2020.e00452>
 8. Siwek H, Bartkowiak A, Włodarczyk M. Adsorption of phosphates from aqueous solutions on alginate/goethite hydrogel composite. *Water.* 2019;(11):633. <https://doi.org/10.3390/w11040633>
 9. Alaba O, Johnson O, Leke E. Results in materials thermodynamics and adsorption study of the corrosion inhibition of mild steel by *Euphorbia heterophylla L.* extract in 1.5 M HCl. *Res Mat.* 2020;(5):100074. <https://doi.org/10.1016/j.rinma.2020.100074>
 10. Abdelhay A, Al Bsoul A, Al-Othman A et al. Kinetic and thermodynamic study of phosphate removal from water by adsorption onto (*Arundo donax*) reeds. *Ads Sci Tech.* 2018;(36):46-61. <https://doi.org/10.1177/026361746684347>
 11. Ayoola AA, Fayomi OSI, Akande IG et al. Inhibitive corrosion performance of the eco-friendly *Aloe vera* in acidic media of mild and stainless steels. *J Bio Tribo Corros.* 2020;(6):1-13. <https://doi.org/10.1007/s40735-020-00361-y>
 12. Popoola API, Sanni O, Loto CA et al. Corrosion inhibition: synergetic interactions of corrosion inhibition tendency of two different gluconates on mild steel in different corrosive environments. *Port Electrochim Acta.* 2015;(33):353-370. <https://doi.org/10.4152/pea.201506353>
 13. Muryanto S, Hadi SD. Adsorption laboratory experiment for undergraduate chemical engineering: Introducing kinetic, equilibrium and thermodynamic concepts. *Conf Series: Mat Sci Eng.* 2016;(162):012004. <https://iopscience.iop.org/article/10.1088/1757-899X/162/1/012004>
 14. Yiase SG, Adejo SO, Tyohemba TG et al. Thermodynamic, kinetic and adsorptive parameters of corrosion inhibition of aluminum using sorghum bicolor leaf extract in H₂SO₄. *IJARCS.* 2014;(1):38-46. <https://www.arcjournals.org/pdfs/ijarcs/v1-i2/6.pdf>
 15. Ibrahim M B, Jimoh W L. Thermodynamics and adsorption isotherms for the biosorption of Cr (VI), Ni (II) and Cd (II) onto maize cob. *Chem Search J.* 2012;(3):7-12. <https://www.ajol.info/index.php/csj/issue/view/12136>
 16. Odunlami OA, Abatan OG, Busari AA et al. Electrochemical control of high carbon steel corrosion using rosemary oil in citric acid medium. *IOP Conf Series: Mat Sci Eng.* 2012(1036):012051. <https://doi.org/10.1088/1757-899X/1036/1/012051>